

Journal Pre-proofs

Pseudomonas aeruginosa host-pathogen interactions in human corneal infection models

Ahmad Elsahn, Maria del Mar Cendra, Maria Victoria Humbert, Myron Christodoulides, Harminder Dua, Parwez Hossain

PII: S2452-4034(20)30003-0
DOI: <https://doi.org/10.1016/j.xjec.2020.02.002>
Reference: XJEC 25

To appear in: *Journal of EuCornea*

Received Date: 3 February 2020
Accepted Date: 26 February 2020

Please cite this article as: A. Elsahn, M. del Mar Cendra, M.V. Humbert, M. Christodoulides, H. Dua, P. Hossain, *Pseudomonas aeruginosa* host-pathogen interactions in human corneal infection models, *Journal of EuCornea* (2020), doi: <https://doi.org/10.1016/j.xjec.2020.02.002>

This is a PDF file of an article that has undergone enhancements after acceptance, such as the addition of a cover page and metadata, and formatting for readability, but it is not yet the definitive version of record. This version will undergo additional copyediting, typesetting and review before it is published in its final form, but we are providing this version to give early visibility of the article. Please note that, during the production process, errors may be discovered which could affect the content, and all legal disclaimers that apply to the journal pertain.

© 2020 Published by Elsevier Inc. on behalf of European Society of Cornea & Ocular Surface Disease Specialists.



Title: *Pseudomonas aeruginosa* host-pathogen interactions in human corneal infection models

Authors: Ahmad Elsahn^{1,2,3¶}, Maria del Mar Cendra^{2¶}, Maria Victoria Humbert², Myron Christodoulides², Harminder Dua^{1*}, Parwez Hossain^{2,3*}

Affiliations:

1. Academic Ophthalmology, Division of Clinical Neurosciences, School of Medicine, University of Nottingham, Nottingham, United Kingdom
2. Molecular Microbiology, Division of Clinical and Experimental Sciences, Faculty of Medicine, University of Southampton, Southampton, United Kingdom
3. Southampton Eye Unit, University Hospitals Southampton NHS Foundation Trust, Southampton, United Kingdom

¶Equally contributing authors

*Equally contributing corresponding authors

Author for correspondence: Harminder.dua@nottingham.ac.uk

Running title: *Pseudomonas aeruginosa* keratitis in human tissue model

Keywords: cornea, pseudomonas aeruginosa, keratitis, corneal fibroblasts.

Address for correspondence:

Academic Ophthalmology

Division of Clinical Neurosciences

School of Medicine

University of Nottingham

E/B 5063, B Floor, EENT building

Queen's Medical Centre

Derby Road, Nottingham NG7 2RD United Kingdom

Synopsis

P. aeruginosa bacteria only penetrate corneal epithelium when it is breeched or bypassed. They can colonize the stroma and internalize into keratocytes, surviving and replicating inside them, which can lead to persistence and reactivation of infection

Abstract

Purpose: To examine over time, the electron microscopic changes associated with *Pseudomonas aeruginosa* (PA) and human corneal tissue interactions in the context of microbial keratitis.

Methods: Corneal stromal fibroblast monolayer and whole tissue models were made from human eye bank eyes and from residual tissue after corneal transplantation.

In the whole tissue model (WTM), donor buttons were infected with PAO1 by scoring and intrastromal injection. Tissue was examined after 3, 9 and 24 hours post challenge by transmission electron microscopy (TEM) and scanning electron microscopy (SEM).

In the cell culture model (CCM), corneal fibroblasts (CF) were infected in vitro with PAO1.

Bacterial adherence and internalization were assayed at 3, 6 and 9h by SEM and TEM.

Adherent and internalized bacteria were measured by the gentamicin protection invasion assay. A subset of infected fibroblasts was treated with gentamicin to study intracellular bacterial survival and cell viability using a lactose dehydrogenase assay (LDH).

Results: In the WTM, bacteria were seen to penetrate the epithelium at the scored sites only. At 3h bacteria were seen in the stroma and by 9h distinct intrastromal bacterial colonies were observed. Clusters of intracellular bacteria were observed in keratocytes in the intrastromal injection model.

In CCM, SEM demonstrated bacteria adherent to the surface of CF and the saponin lysis assay demonstrated adherence and internalization in a dose- and time-dependent manner. Bacterial internalization was detected as early as 3h. Intracellular bacteria survived and replicated without affecting cell viability.

Conclusion: PAO1 bacterial can infect stromal keratocytes only when the epithelium and basement membrane are breached, or bypassed by direct injection. PA interaction with CF occurs very early leading to internalization of bacteria where they are protected and can multiply intracellularly without affecting CF viability for 24 hrs. This may have relevance to ideal timing of medical intervention.

Introduction

Microbial keratitis remains a significant public health problem as a major cause of visual disability around the world, and yet it is alarmingly under-diagnosed and under-treated ¹.

There is an estimated 1.5-2 million people that develop corneal ulceration every year in developing countries,² and as much as 40% of childhood and 20% of adult corneal blindness are caused by infectious keratitis. Corneal infections, including trachoma, were the leading cause of unilateral and bilateral corneal blindness in some areas ^{3 4}.

Contact lens wear accounts for up to 50.3% of cases of microbial keratitis ⁵ in the western world, and *Pseudomonas aeruginosa* is the most commonly isolated causative organism for contact lens associated microbial keratitis, accounting for up to 68.8% of isolates ⁶⁻¹¹. *P.*

aeruginosa microbial keratitis is one of the most devastating, rapidly progressing corneal infections, which can cause corneal perforation, endophthalmitis and, ultimately, blindness.

Numerous live animal models of microbial keratitis have been developed to study the effects of bacterial colonization and virulence factors, the host responses to the pathogen and the interplay between bacterium and host. In the vast majority of these models, the corneal epithelium is bypassed either by scoring it down to the epithelial basement membrane, or by directly injecting bacteria into the stroma. This is because in the healthy cornea, the intact corneal epithelium is a formidable barrier to invasive microbial keratitis, and only when the bacteria reach the corneal stroma, does a corneal ulcer develop. A number of animal studies have investigated the ultrastructural host-pathogen interactions that occur in microbial keratitis, but these have not been replicated in human tissue.

Although these animal models are fairly representative of the pathology, they are limited by the significant differences in the morphology and dimensions between, for example, murine and human corneas ¹². In addition, the pharmacokinetics of substances is different in

humans from all laboratory animal species, and there are considerable differences in metabolic rates, body temperature, elimination routes, carrier proteins/protein binding, and defence mechanisms ¹³.

Apart from interactions with the host immune cells, invading organisms affect the resident corneal epithelial cells and keratocytes. The response of these cells to the microbes is the forerunner for the immune response that follows. In vitro and ex-vivo models do not allow the study of the immune cell response, but this is an advantage when it comes to studying specific responses of the resident cells, as the picture is not compounded by the infiltrating inflammatory cells. In the current study, we designed in vitro and ex-vivo models of microbial keratitis using human whole tissue and cell culture environments to undertake an ultrastructural examination of host-pathogen interactions in a sequential manner.

Materials and Methods

Human corneal tissue and cell culture

Donor human corneal buttons (hCB), whole corneas and corneo-scleral rims remaining after endothelial and penetrating keratoplasty procedures were collected. Ethics Committee approval was obtained (ethics number 06/Q1602/56). The study adhered to the tenets of the Declaration of Helsinki. Corneal tissue samples were processed within 5 days of collection. Donor age range was 63-87 years with a mean age of 68 years. The causes of death were cancer, cardiac, infections, pulmonary, neurological and others.

For the whole tissue model, whole corneas or corneal buttons obtained after Descemet's stripping endothelial keratoplasty (DSEK; epithelium and anterior stroma without Descemet's membrane and endothelium) were used. For the cell culture model, primary human corneal fibroblasts (keratocytes) (hCF) were isolated as described previously¹⁴.

Briefly, the epithelium was scraped off the corneo-scleral rims, the rims divided into small sections of 2-3 mm each and the samples were incubated in 5 ml culture medium with 1 mg/ml collagenase (from *C. histolyticum*, Sigma-Aldrich, Dorset, UK) for 3h at 37°C.

Thereafter the suspension was centrifuged at 72 *g* for 1 min, and the pellet was suspended in 10 ml of culture medium in 25ml flasks. The flasks were incubated for 3-4 days until the cells were confluent at the bottom of the flask, trypsinized, resuspended and expanded in fresh medium for 3-4 passages. For TEM and SEM studies, hCF were grown to confluence on collagen pre-coated transwells (ThinCerts™, transparent pore size 0.4 µm; Greiner Bio-one, Stonehouse, UK) in the final passage. Polymerase chain reaction (PCR) was used to confirm the absence of *Mycoplasma* contamination.

Bacterial Culture and infection of human corneal tissue

P. aeruginosa wild type strain PAO1 Holloway1C Stanier131 was obtained from NCIMB (Aberdeen, UK) and stored at -80°C. Prior to each experiment, bacteria were grown overnight on nutrient agar (Oxoid, UK) in an incubator at 37°C, 5% (v/v) CO₂. From this a bacterial suspension was prepared to attain an optical density (OD) (Hitachi U-1100 spectrophotometer, Hitachi, Tokyo, Japan) equal to an infective dose of 10⁷ CFU/mL.

Ex-vivo model. Two methods of infection were used: the intra-stromal or the trans-epithelial methods. In the intra-stromal method, 50 µL of infective solution were injected into the corneal stroma from the endothelial side using a 30 gauge needle. The whole corneas were incubated in culture medium [DMEM F12 medium with 2% FBS] at 37°C for 24h. Thereafter, the corneas were washed 4 times in warm sterile PBS and processed for electron microscopy. In the trans-epithelial method, two buttons were used. One button was scarified by a 27 gauge needle to produce 4-5 linear epithelial scores that were deep enough to bypass the epithelium and score the underlying stroma. The other button was left with an intact epithelium and used as control.

TEM studies: A five-millimetre corneal trephine was inserted into the centre of each corneal button (scored and unscored) through at least half the thickness of the button so that the hollow of the trephine acted as a well in which the infective medium was placed. The corneas with the trephines were then immersed in culture medium, such that the cornea was submerged in the medium but the trephine acted as a barrier avoiding contact between the infective medium in the well and the culture medium outside of it. This was incubated at 37°C for 9h.

SEM studies: Two buttons were used. One button was scored and divided into two halves. One half was infected and the other not. The unscored button was similarly treated yielding

one half that was infected and the other not. Infection was achieved by immersing the buttons in infected medium while the non-infected controls were immersed in clean culture medium.

Cell culture model. For SEM and TEM studies 1 mL of infective solution was added to each transwell containing a confluent monolayer of hCF. The plates were incubated in 5% (v/v) CO₂ at 37°C for 3 to 24h. The cells were fixed and processed for electron microscopy. For association and invasion studies, 1 mL of infective solution was added to each monolayer-containing well, and the plates were incubated in 5% (v/v) CO₂ at 37°C for 3 to 24h.

Scanning Electron Microscopy (SEM)

For the cell culture model, the cells were rinsed with sterile PBS and then processed for SEM. Transwells were fixed for a minimum of 1h using a fixative solution [3% (v/v) glutaraldehyde and 4% (v/v) formaldehyde in 0.1 M PIPES (1,4-Piperazine diethanesulfonic acid) buffer pH 7.2] and were rinsed twice in buffer solution (0.1 M PIPES buffer) for 10min each. The transwell membranes were detached and subjected to dehydration using graded concentrations of ethanol from 30%, 50%, 70%, 95% and up to 100% (v/v) solutions, 10min for each step and 20min for the final step. The membranes were critical-point dried and mounted on to metal stubs for the final sputter coating step. Coated specimens were viewed using the Quanta 200 scanning electron microscope (FEI, Hillsboro, USA) and several images were obtained for each specimen at magnifications of x3200 and up to x24000. A similar method was used for the whole tissue model using hCB instead of hCF membranes.

Transmission Electron Microscopy (TEM)

Human corneal tissue (hCB and hCF) were processed in a manner similar to that described for SEM above, until the ethanol dehydration step. The samples were incubated overnight, on a rotor (2rpm), in spur resin at a 50:50 ratio with acetonitrile. After that, the samples

were placed in fresh spur resin and polymerised in an electric oven at 60°C for 20-24h. In preparation for microscopy, sample blocks were cut into ultrathin sections (about 90 nm thick) using glass knives on a Leica Reichert Ultracut E microtome (Leica, Wetzlar, Germany). Several sections per sample were fixed on to copper grids and stained using lead nitrate for 5min in the presence of NaOH crystals. The grids were briefly rinsed in distilled water and air dried. Sample viewing was done using either a H7000 transmission electron microscope (Hitachi, Japan) at 75Kv or a Tecnai T12 BioTwin transmission electron microscope (Hillsboro, OR, USA) at 100kV. Images were captured using a Megaview III Soft Imaging System (SIS) camera.

Assessment of bacterial association to and invasion of corneal fibroblasts

To quantify bacterial association to hCF, monolayers were challenged in triplicate in 24 well plates with multiplicity of infection (MOI) of bacteria to cells of 0.0001-1000 (Table 1). Total bacterial association was quantified over time using the viable counting and saponin lysis method, as described previously¹⁵. Briefly, hCF monolayers were challenged in triplicate with a MOI of 0.001, 0.1 and 100 and incubated at 37°C for 3, 6, 9 and 24h. Cell monolayers were gently rinsed with warm PBS and attached bacteria were released using a saponin solution [10 mL PBS containing 1% (w/v) saponin powder and 1% (v/v) decomplexed foetal bovine serum]. The saponised lysates were inoculated on agar plates, incubated at 37°C for 24h and colony-forming units (CFU) were quantified using a ProtoCOL model 60000 automated colony counter (Synoptics Ltd, Cambridge, UK).

Bacterial invasion was quantified as described previously¹⁶. Briefly, confluent hCF monolayers were challenged in triplicate with a MOI of 100 and incubated at 37°C for 3h. Cell monolayers were rinsed with PBS and then 1ml of medium containing 200 µg/ml of gentamicin (Sigma-Aldrich, Dorset, UK) was added to the wells and incubated at 37°C for

90min. Monolayers were washed with PBS and intracellular bacteria were released using a saponin solution, and bacteria were quantified by viable counting on nutrient agar plates. Bacterial association and invasion were assessed simultaneously in different wells. Wells treated with gentamicin yielded invaded bacteria only and wells not treated with gentamicin yielded both attached and invaded bacteria.

Confocal Microscopy

To analyse actin stress fibres, hCF monolayers were infected for 3h with Green Fluorescent Protein (GFP)-expressing PAO1 wild-type bacteria (MOI=100). Monolayers were washed with PBS and fixed with paraformaldehyde (4% v/v) for 15min at RT. Cells were permeabilised with PBS containing 0.1% (v/v) saponin and 10% (v/v) decompemented fetal calf serum (dFCS) for 2h at 4°C and then counter-stained with Rhodamine-phalloidin (1/50 v/v) (Thermo-Fisher Scientific) for 30min at RT, protected from light. After counterstaining, hCF monolayers were washed with PBS and examined with a Leica TCS SP8 DLS confocal microscope. When required, images were optical zoomed within the Nyquist limits (ref: Nyquist, H Trans. AIEE 1928) in order to have the largest acceptable pixel sizes to precisely determine the stress fibbers disruption promoted by PAO1 in hCFs.

Immunoprecipitation and western blot analysis

The RhoA/Rac1/Cdc42 Activation Assay Combo Biochem kit™ (Cytoskeleton, Inc) was used according to the manufacturer instructions. hCF monolayers were grown in DMEM containing 1% (v/v) dFCS and at 70% confluence, the medium was changed to serum-free medium. Serum-starved monolayers were infected with wild-type PAO1 for 1h (MOI=100) and total protein was extracted. Equal amounts of total protein extract was used to immunoprecipitate RhoA, Rac1 and Cdc42 total protein independently using rhotekin-RBD and PAK-PBD affinity beads, loaded onto a 12% (w/v) SDS-PAGE gel and transferred onto PVDF membranes (GE Healthcare). GTPase activation was examined with mouse monoclonal anti-RhoA, -Rac1 and -Cdc42 antibodies supplied in the kit and used at the recommended dilutions. Goat anti-Mouse IgG (H+L)-HRP Conjugate (Bio-Rad) was used as a secondary antibody at the recommended dilution.

To assess Src-kinase protein expression, total protein was extracted from hCF monolayers infected for 6h with PAO1 wild-type strain (MOI=10). Total protein (5µg) was separated by 12% (w/v) SDS-PAGE and transferred onto PVDF membranes. Polyclonal Src antibody ab7950 and anti-Src[pY418] (Abcam) were used to detect non-phosphorylated and phosphorylated Src, respectively. Goat anti-Rabbit IgG H&L HRP pre-adsorbed secondary antibody (Abcam) was used according to the manufacturer's recommendations. Immuno-detection was carried out in a Versadoc 4000 (BioRad) and data analysed with Quantity One 4.6.9 software (BioRad).

Inhibitors

When required, genistein (50µM, Sigma-Aldrich), PP2 (10µM, Sigma-Aldrich) or Rhosin (30µM and 50µM, Merck Millipore) was added to the monolayers, 30min prior to infection.

Cell viability assessment

Cell viability was quantified using a Lactate dehydrogenase (LDH) assay (CytoTox 96® Non-Radioactive Cytotoxicity assay kit, Promega, Madison, WI, USA). Confluent fibroblast monolayers were challenged with bacteria for 90min before adding gentamicin. Cytotoxicity levels were calculated by dividing the average LDH release value of test samples by the average maximum LDH release value from lysed uninfected cells.

Statistical Analysis

Statistical analysis was done using SPSS version 22.0 (IBM, Armonk, NY, USA). For comparison between two groups, an unpaired Student's t-test was used. For non-normal distributions, the Mann-Whitney rank sum test was used. To determine the difference in the frequency of infection between hCB groups, a χ^2 test was used.

Results

The corneal epithelium is a formidable barrier against infection

SEM of corneal buttons showed that, unlike the smooth surface and the minimal exfoliation of superficial epithelial cells in control samples, the epithelial surface appeared much rougher in corneas infected with PAO1 bacteria for 3h (Figure 1A-D). The number of exfoliating cells was also higher; in a given area of 60x60 μm , 21 exfoliating cells were seen in the infected cornea versus 11 in the control sample. With higher magnification, *P. aeruginosa* bacteria were seen adhering to exfoliating epithelial cells (Figure 1E), and some bacteria seemed to be penetrating the epithelial cell surface (Figure 1F).

In a light microscopic section of scarified hCB, it was evident that the scores had bypassed the epithelial basement membrane into the stroma. Epithelial cells seemed to migrate to fill the gap (Figure 2A). In the TEM of the non-scarified hCB, the bacteria were seen in all layers of epithelium but not beyond the basement membrane (BM). They were seen to line up on the epithelial side (Figure 2B) of the BM. In the scarified button, the area of the epithelial score showed epithelial cells and PAO1 bacteria within the score and invading the adjacent stroma (Figure 2C and D). At the later time point of 9 hours bacteria appeared to aggregate within the stroma forming small colonies (Figure 2E and F). At 24h, bacteria were found to accumulate inside stromal keratocytes, with occasional bacteria in the surrounding stroma (Figure 2G-I).

P. aeruginosa bacteria adhere to and invade human corneal fibroblasts

Bacterial adherence was demonstrated by SEM. Bacteria were seen adhering to the surface of the fibroblasts, with a greater number of adherent bacteria observed with higher MOI (Figure 3B and C). This was confirmed by the saponin bacterial association assay. The bacteria showed a linear dose-dependent association with hCF monolayers over time (MOI

0.0001, 0.001, 0.01 and 0.1 - Figure 3A). This demonstrates that bacterial association to corneal fibroblasts is a normal, repeatable host-pathogen interaction not occurring by chance. Infection with MOI 10, 100 and 1000 led to a rapid saturation of the monolayers and monolayer destruction by 9-24h.

Bacterial internalization was demonstrated by TEM. Bacteria were detected in apposition to the surface of corneal fibroblasts (Figures 4A), with a cup-like invagination from the surface of the fibroblast and within cell-bound vacuoles completely inside host cells (Figures 4B and C). This was confirmed by the gentamicin protection invasion assays. Bacterial invasion of corneal fibroblasts was detectable by 9h post challenge at lower MOI (0.001 and 0.1), and by 3h at higher MOI (100). Cytochalasin D, a cell-permeable inhibitor of actin polymerization, reduced the number of internalized bacteria, but had no significant effect bacterial adherence to fibroblasts in any of the infective doses or time points (Figure 4D-F).

An invasion index was calculated and expressed as a percentage of the total number of associated bacteria. The rate of invasion was concomitantly higher with a higher infecting dose and a shorter duration of infection, with a geometric mean level of invasion ($\pm 95\%$ confidence limits) of 1.4% (0.68, 2.87%); in comparison to lower infecting doses and prolonged infection periods, with 0.3% (0.04, 2.61%) infection. However, this difference was not statistically significant ($P > 0.05$).

Protein tyrosine kinases (PTK) are involved in bacterial internalisation into corneal fibroblasts

A molecular analysis of PAO1 invasion pathway was done to explain the temporal phenotypic changes induced as a response to hCF infection. Protein tyrosine kinases (PTKs) are considered to be important for bacterial invasion of mammalian cells¹⁷. Specifically, Src kinases are involved in the signalling pathway downstream the bacterial-stimulated integrins¹⁸. To determine the involvement of PTKs in PAO1 uptake by hCFs, genistein (50 μ M) was used to block total PTKs, and PP2 (10 μ M) to inhibit Src kinase during PAO1 invasion. There was a significant ~ 2 log reduction in hCF invasion by PAO1 ($P < 0.0001$) with both genistein- and PP2-treated hCF compared to untreated cells ($P < 0.0001$) (Figure 5A). Human Src kinases are composed of a N-terminal SH3 and SH2 kinase domain and a C-terminal regulatory tyrosine residue (Y₅₂₉). When the C-terminal-tyrosine is dephosphorylated, a change in protein conformation promotes trans-autophosphorylation of Y₄₁₈ that allows kinase activation¹⁹⁻²². Phosphorylation and consequent activation of Src kinase during PAO1 hCF-invasion was confirmed by western blot analysis. Protein band densitometry relative to β -actin revealed a significant $\sim 87.5\%$ induction of total Src protein, $\sim 53\%$ of which was phosphorylated, as a percentage of total Src kinase induction, in hCF infected with PAO1 and differently to non-infected monolayers, in which no Src protein could be detected (Figure 5B).

RhoA, Rac1, and Cdc42 are Rho family small GTPases involved in signalling pathways for cytoskeleton actin rearrangements^{23 24}. RhoA, Rac1 and Cdc42 proteins were immunoprecipitated from PAO1-infected hCFs and protein levels analysed by western blot. The three GTPases were identified in PAO1-infected hCF, but only RhoA showed the GTP bound activation state. Even though RhoA activation was observed in uninfected hCFs, protein

band densitometry relative to uninfected condition revealed ~52% induced RhoA-GTP in infected hCF compared to control (uninfected) monolayers (Figure 6A). RhoA involvement in PAO1 hCF uptake was confirmed by analysing bacterial invasion following RhoA inhibition with Rhosin. RhoA inhibition significantly reduced PAO1 invasion of hCF in a Rhosin dose-dependent manner ($P < 0.01$ with $30\mu\text{M}$ Rhosin and $P < 0.001$ with $50\mu\text{M}$ Rhosin) (Figure 6B). Confocal microscopy confirmed the disassembly of stress fibres promoted by PAO1 activation of RhoA during hCF invasion. The intensity of stress fibres detected after infection with PAO1 wild-type strain decreased and cell arches disappeared, compared to the long and well-developed stress fibres observed in control monolayers. Nyquist sampling confirmed stress fibre disruption in PAO1-infected hCFs (Figure 6C).

***P. aeruginosa* bacteria use corneal fibroblasts as reservoirs for protection and reinfection**

In both the cell culture and the whole tissue TEM studies, bacteria were seen clustered inside corneal fibroblasts. In the subset of fibroblast monolayers that were treated with gentamicin 3h post challenge, all extracellular bacteria were destroyed but the number of bacterial recovered after 24hours had significantly increased suggesting that surviving PAO1 bacteria replicated inside corneal fibroblasts (Figure 7). Samples of supernatant taken after 24 hours showed no bacterial growth. Control samples showed no effect of gentamicin on non-infected cells as has been previously demonstrated.

The LDH assay showed that infected fibroblasts without antibiotic treatment released significantly more LDH (~50-100%) than uninfected cells ($p < 0.05$). However, there was no significant difference between the levels of LDH released from hCF with intracellular bacteria treated with gentamicin and uninfected cells at 9 or 24h ($P > 0.05$), suggesting that cell viability was not affected by the presence of intracellular bacteria (Figure 8).

Discussion

Early studies of PA microbial keratitis show progressive destruction and liquefaction of the cornea that rapidly leads to perforation unless intense antibiotic treatment is immediately initiated ²⁵. This has long been noticed in clinical practice, and patients presenting with suspected microbial keratitis are immediately started on intensive topical antibiotic treatment, without waiting for culture and sensitivity results, which when available are used to modify treatment if there is an insufficient response. Clinically it is known that infected corneal ulcers require immediate treatment but the exact duration is difficult to quantify.

This study was conducted to ascertain how rapidly bacteria interact with corneal tissue cells and propagate through the cornea. Although the surface epithelial cells desquamate to reduce the bacterial load and the epithelial basement membrane prevents further propagation of bacteria into the stroma, bacteria colonise the stroma and rapidly interact with corneal fibroblasts when there is a breach in defences. They adhere to and invade the cells as early as 3h and destroy them by 9h, or they can survive and replicate intracellularly without affecting cell viability, using fibroblasts as reservoirs for self-protection and re-infection.

The normal wound healing response observed in our whole tissue model demonstrated that this was a viable model for this study. When corneal buttons were infected with *P. aeruginosa*, they showed a rougher epithelial surface and greater levels of desquamating cells than uninfected buttons, which is consistent with findings in a rat model, where most internalized bacteria were found in cells that were readily desquamated from the cornea with rinsing ²⁶. This indicates that the internalization/desquamation sequence is a defence mechanism that the human cornea also employs to reduce the bacterial load. We also showed that *P. aeruginosa* successfully adhered to corneal epithelial cells, and managed to penetrate the entire epithelium but could not penetrate further into the stroma unless there was a breach in the epithelial basement membrane, or when injected directly into the stroma. This is consistent with studies utilizing mouse models showing

similar findings²⁷. Thus, although these bacteria can invade intact epithelium, they penetrate the basement membrane with difficulty.

In the stroma, *P. aeruginosa* bacteria rapidly interact with corneal fibroblasts, and are able to colonize the stroma quite efficiently. In our model, PAO1 bacteria adhered to corneal fibroblasts in a linear dose- and time-dependant manner, starting as early as 3h post challenge, and increasing progressively with time. Our results also showed that *P. aeruginosa* internalisation into corneal fibroblasts could be detected as early as 3h post challenge, where bacteria entered cells by endocytosis and resided in cytosolic vesicles.

Bacterial internalisation by corneal fibroblasts appears to be an important host-pathogen interaction, which could confer survival advantage to the bacteria. Internalised bacteria can survive and replicate inside invaded fibroblasts without affecting fibroblast viability for up to 24h. Apart from directly colonising the stroma, bacteria also cluster inside stromal keratocytes. This indicates that, although in a clinical scenario bacteria do not particularly need to invade corneal fibroblasts in order to traverse the stroma, they may well use this internalization to evade host defences and instilled antibiotics. This is sometimes noticed clinically, when ulcers remain active despite antibiotic treatment, and when a “responding ulcer” flares up on withdrawal or reduction in frequency of instillation of the antibiotic. In a retrospective review of therapeutic keratoplasty in Singapore²⁸, *P. aeruginosa* accounted for 58.7% of refractory microbial keratitis requiring penetrating keratoplasty. Interestingly, all patients were treated initially with gentamicin and cefazolin, and then other modalities were tried when the ulcers were progressively worsening. It is possible that in those patients, bacteria would have survived intracellularly, safe from gentamicin, and reached a critical threshold when they externalised, probably through cellular disruption of fibroblasts/kertocytes. The large number of externalised bacteria would overwhelm host defences and perpetuate infection.

In our model we were able to replicate in human tissue, observations made in animal models.

Although many investigators have used mouse models to study the pathology of microbial keratitis, the mouse cornea has many structural and morphological differences to the human cornea. It is

much smaller, with a diameter of 2.3-2.6 mm, compared to 11-13 mm in humans, and much thinner, measuring 122-137 μm , compared to 550 μm on average in humans. The murine epithelium represents one third of the corneal thickness compared to one tenth in humans, and is composed of 13 layers of cells with multiple layers of squamous cells, compared to 5-6 layers in humans. There is also no distinct epithelial basement membrane and Bowman's layer, but rather a much less well-developed anterior limiting lamina separating the epithelium from the stroma. Finally, the anterior stroma does not show the dense and complex interweaving of collagen fibres seen in human corneas.¹² By using our human tissue derived models, the ultrastructural host-pathogen interactions can be accurately described in the context of human tissue and closely resemble changes in real-life clinical scenarios.

Our model has a number of limitations. A significant part of the morbidity associated with microbial keratitis is attributable to the host immune response, and our model lacks the presence of immune cells, which are pivotal in the pathogenesis of microbial keratitis. Our model is more reflective of changes occurring in infectious crystalline keratopathy, where the local host immune response is compromised. Further studies using these models with the introduction of immune cells to simulate microbial keratitis more closely, may provide more relevance. We used one laboratory strain of *P. aeruginosa* (PAO1), which might behave differently than clinical isolates. The models are also amenable to further studies using pathogenic clinical isolates from patients with corneal ulcers.

The sequence of events observed in this study provides a useful temporal insight into the ultrastructural changes that accompany the host-pathogen interactions in corneal cells. This information is of relevance to the progression of microbial keratitis and can provide some understanding of the pathogenesis of keratitis and timing of medical intervention.

Acknowledgement

We would like to acknowledge Professor Tim Tolker-Nielsen and his group for their support and collaboration. We acknowledge the staff of the Imaging and Microscopy Centre at the University of Southampton for their valuable support. We also thank the Nanoscale and Microscale Research Centre (nmRC) at the University of Nottingham for providing access to instrumentation, and Denise McLean (School of Life Sciences) for technical assistance

Author contributions

AE, MC, MDMC and PH have conceived and designed the experiments

AE and MDMC performed the experiments and analysed the results

AE, MDMC, MC, PH and HD have written the manuscript and approved the final draft

PH and HD are equally contributing corresponding authors

AE and MDMC are equally contributing authors of the study.

Financial support:

1. The British Council for the Prevention of Blindness
2. The Royal College of Surgeons of Edinburgh
3. The National Eye Research Centre

The funding organisations had no role in the conception, design or conduct of this research

Financial disclosures:

Professor Dua has the following disclosures: Consultant adviser to Croma, Chiesi, Santen, Thea, Visufarma (travel, expenses, honoraria), shares in Glaxosmithkline and NuVision biotherapeutics. No conflicting relationship exists for any other author.

References

- Whitcher JP, Srinivasan M. Corneal ulceration in the developing world--a silent epidemic. *Br J Ophthalmol* 1997;81(8):622-3.
- Garg P, Krishna PV, Stratis AK, et al. The value of corneal transplantation in reducing blindness. *Eye* 2005;19(10):1106-14. doi: 10.1038/sj.eye.6701968
- Rapoza PA, West SK, Katala SJ, et al. Etiology of corneal opacification in central Tanzania. *International ophthalmology* 1993;17(1):47-51.
- Bowman RJ, Faal H, Dolin P, et al. Non-trachomatous corneal opacities in the Gambia--aetiology and visual burden. *Eye* 2002;16(1):27-32. doi: 10.1038/sj.eye.6700027
- Bourcier T, Thomas F, Borderie V, et al. Bacterial keratitis: predisposing factors, clinical and microbiological review of 300 cases. *The British journal of ophthalmology* 2003;87(7):834-8.
- Hoddenbach JG, Boekhoorn SS, Wubbels R, et al. Clinical presentation and morbidity of contact lens-associated microbial keratitis: a retrospective study. *Graefe's archive for clinical and experimental ophthalmology = Albrecht von Graefes Archiv fur klinische und experimentelle Ophthalmologie* 2014;252(2):299-306. doi: 10.1007/s00417-013-2514-1 [published Online First: 2013/11/28]
- Tabbara KF, El-Sheikh HF, Aabed B. Extended wear contact lens related bacterial keratitis. *The British journal of ophthalmology* 2000;84(3):327-8. [published Online First: 2000/02/24]
- Patrinely JR, Wilhelmus KR, Rubin JM, et al. Bacterial keratitis associated with extended wear soft contact lenses. *The CLAO journal : official publication of the Contact Lens Association of Ophthalmologists, Inc* 1985;11(3):234-6. [published Online First: 1985/07/01]
- Galentine PG, Cohen EJ, Laibson PR, et al. Corneal ulcers associated with contact lens wear. *Archives of ophthalmology (Chicago, Ill : 1960)* 1984;102(6):891-4. [published Online First: 1984/06/01]
- Shah A, Sachdev A, Coggon D, et al. Geographic variations in microbial keratitis: an analysis of the peer-reviewed literature. *The British journal of ophthalmology* 2011;95(6):762-7. doi: 10.1136/bjo.2009.169607 [published Online First: 2011/04/12]
- Jeng BH, Gritz DC, Kumar AB, et al. Epidemiology of ulcerative keratitis in Northern California. *Archives of ophthalmology (Chicago, Ill : 1960)* 2010;128(8):1022-8. doi: 10.1001/archophthalmol.2010.144 [published Online First: 2010/08/11]
- Henriksson JT, McDermott AM, Bergmanson JP. Dimensions and morphology of the cornea in three strains of mice. *Invest Ophthalmol Vis Sci* 2009;50(8):3648-54. doi: 10.1167/iovs.08-2941 [published Online First: 2009/03/07]
- Hartung T. Thoughts on limitations of animal models. *Parkinsonism & related disorders* 2008;14 Suppl 2:S81-3. doi: 10.1016/j.parkreldis.2008.04.003 [published Online First: 2008/07/01]
- Wong Y, Sethu C, Louafi F, et al. Lipopolysaccharide regulation of toll-like receptor-4 and matrix metalloprotease-9 in human primary corneal fibroblasts. *Invest Ophthalmol Vis Sci* 2011;52(5):2796-803. doi: 10.1167/iovs.10-5459
- Alkuwaity K, Taylor A, Heckels JE, et al. Group B Streptococcus interactions with human meningeal cells and astrocytes in vitro. *PLoS one* 2012;7(8):e42660. doi: 10.1371/journal.pone.0042660 [published Online First: 2012/08/18]
- Hardy SJ, Christodoulides M, Weller RO, et al. Interactions of Neisseria meningitidis with cells of the human meninges. *Molecular microbiology* 2000;36(4):817-29. [published Online First: 2000/06/09]
- Rosenshine I, Duronio V, Finlay BB. Tyrosine protein kinase inhibitors block invasin-promoted bacterial uptake by epithelial cells. *Infection and immunity* 1992;60(6):2211-7. [published Online First: 1992/06/01]
- Leroy-Dudal J, Gagniere H, Cossard E, et al. Role of alphavbeta5 integrins and vitronectin in Pseudomonas aeruginosa PAK interaction with A549 respiratory cells. *Microbes and infection / Institut Pasteur* 2004;6(10):875-81. doi: 10.1016/j.micinf.2004.05.004 [published Online First: 2004/08/18]

19. Schwartzberg PL. The many faces of Src: multiple functions of a prototypical tyrosine kinase. *Oncogene* 1998;17(11 Reviews):1463-8. doi: 10.1038/sj.onc.1202176 [published Online First: 1998/10/21]
20. Xu W, Harrison SC, Eck MJ. Three-dimensional structure of the tyrosine kinase c-Src. *Nature* 1997;385(6617):595-602. doi: 10.1038/385595a0 [published Online First: 1997/02/13]
21. Shattil SJ. Integrins and Src: dynamic duo of adhesion signaling. *Trends in cell biology* 2005;15(8):399-403. doi: 10.1016/j.tcb.2005.06.005 [published Online First: 2005/07/12]
22. Lieser SA, Shindler C, Aubol BE, et al. Phosphoryl transfer step in the C-terminal Src kinase controls Src recognition. *The Journal of biological chemistry* 2005;280(9):7769-76. doi: 10.1074/jbc.M411736200 [published Online First: 2004/12/30]
23. Nobes CD, Hall A. Rho, rac, and cdc42 GTPases regulate the assembly of multimolecular focal complexes associated with actin stress fibers, lamellipodia, and filopodia. *Cell* 1995;81(1):53-62. [published Online First: 1995/04/07]
24. Moon SY, Zheng Y. Rho GTPase-activating proteins in cell regulation. *Trends in cell biology* 2003;13(1):13-22. [published Online First: 2002/12/14]
25. Kessler E, Mondino BJ, Brown SI. The corneal response to *Pseudomonas aeruginosa*: histopathological and enzymatic characterization. *Invest Ophthalmol Vis Sci* 1977;16(2):116-25. [published Online First: 1977/02/01]
26. Fleiszig SM, Zaidi TS, Pier GB. *Pseudomonas aeruginosa* invasion of and multiplication within corneal epithelial cells in vitro. *Infection and immunity* 1995;63(10):4072-7.
27. Alarcon I, Kwan L, Yu C, et al. Role of the corneal epithelial basement membrane in ocular defense against *Pseudomonas aeruginosa*. *Infection and immunity* 2009;77(8):3264-71. doi: 10.1128/IAI.00111-09
28. Ti SE, Scott JA, Janardhanan P, et al. Therapeutic keratoplasty for advanced suppurative keratitis. *American journal of ophthalmology* 2007;143(5):755-62. doi: 10.1016/j.ajo.2007.01.015 [published Online First: 2007/03/06]

Figure Legends

Figure 1. Interactions of *P. aeruginosa* with human corneal buttons (hCB): bacterial adherence to epithelial cells.

Whole hCB were infected with 10^7 CFU/mL PAO1 bacteria for 3h and 9h before being fixed and processed for SEM. Panels A and B are scans of uninfected buttons; panels C, D, E and F are infected buttons with increasing magnification. Infected buttons demonstrated a rough surface and showed significant desquamation of epithelial cells [C and D] compared to uninfected buttons [A and B]. The arrows point to bacteria adhering to and penetrating the surface of superficial cells [E, F] [Original magnification; A and C= x200, B and D= x1600, E= x5000 and F= x24000].

Figure 2. Interactions of *P. aeruginosa* with human corneal buttons (hCB): Bacterial penetration into corneal stroma.

Whole hCB were infected with 10^7 CFU/mL PAO1 bacteria for 3, 9 and 24h before being fixed and processed for light and transmission electron microscopy (TEM).

Panel A. TEM of unscored area of hCB. Bacteria (white arrows) are seen lined between the epithelial cell and intact basement membrane. Panel B. Light micrograph of a scored corneal button showing epithelial cells filling the score (arrow). Panels C to F. TEM images showing bacteria invading the stroma in increasing magnification (arrows). The bacteria access the stroma only in the scored areas (C, D) and were seen primarily around the scores (Ep = Epithelial cell. S = Stroma). Panels G to I. Bacteria are seen clustered inside stromal keratocytes. [Original magnification; A= x200, C= x1600, D and E= x5000, B and F= x18500, G= x4200, H= x16500, I= x26500]

Figure 3. Dose and time dependent association of *P.aeruginosa* bacteria to human corneal fibroblasts (hCF).

A. hCF monolayers were challenged with 10^7 CFU/mL PAO1 (MOI 100) for 3, 6, 9 and 24h. The association of PAO1 bacteria to corneal fibroblasts was dose- and time-dependant. The symbols represent the mean number of associated bacteria and the error bars the standard error of the mean of 4 independent experiments. With SEM, more bacteria can be seen adherent to fibroblasts (arrows) at MOI 100 (10^7 CFU/mL, B) than MOI 0.1 (10^4 CFU/mL, A). [SEM original magnification= x4000]

Figure 4. Invasion of human corneal fibroblast by low and high infective doses of *P.aeruginosa*

Bacterial internalisation was demonstrated by TEM. Arrows point to bacteria adhering to the cell [A], internalising by endocytosis through a cup like invagination of the fibroblast cell membrane [B], and residing inside the cytoplasm [C]. This was confirmed by a gentamicin protection invasion assay. hCF monolayers were challenged with low infective doses of PAO1 (MOI 0.001 and 0.1) and assessed at 9h post challenge [D and E], and with a higher infective dose (MOI 100) and assessed at 3h post challenge [F]. Cytochalasin D (CD) decreased bacterial invasion but had no effect on bacterial association [A-C]. The bars represent the number of recovered bacteria and the error bars represent the standard error of the mean from 8 independent experiments. [TEM original magnification= x45000 (D), x24000 (E) and x18500 (F)].

Figure 5. *P. aeruginosa* promotes intracellular lifestyle by inducing the PTK family of Src kinase.

(A) PAO1 hCF invasion (denoted with arrows) after 3h at MOI=100 compared to the relative association under non-inhibitory conditions (No treatment), PTKs inhibition with genistein 50 μ M and Src kinases inhibition with PP2 10 μ M. Genistein and PP2 treatment reduce ~98% and ~96% PAO1- hCF invasion compared to invasion in untreated monolayers. Statistical significance is represented by asterisks: *P<0.05; ****P<0.0001. (B) Src kinase, phosphorylated Src-Y418, and β -actin protein levels in hCFs infected with PAO1 wild-type strain for 6h compared to non-infected hCFs. Src kinase protein densitometry relative to endogenous control β actin were 0.15 in uninfected hCFs and 1.20 in PAO1-hCF infection, and for phosphorylated Src-Y418

were 0.18 in uninfected hCF and 0.56 in PAO1-hCF infection. Densitometry calculations were done using the Image LabTM Software (Bio-Rad).

Figure 6. Stress fibres rearrangement by activation of Rho GTPase plays a role during *P. aeruginosa* infection of hCFs.

(A) Total and active GTP-bound protein levels of immunoprecipitated RhoA, Cdc42 and Rac1 from PAO1-infected hCFs, at MOI=100 for 1h, compared to uninfected hCFs. Cdc42- and Rac1-GTP purified protein was used as western blot control. A representative image of n=3 independent experiments is shown. (B) PAO1 hCF invasion under non-inhibitory conditions (No treatment) and with RhoA inhibition with the chemical inhibitor Rhosin at 30 and 50 μ M. Statistical significance is represented by asterisks: **P<0.01; ***P<0.001. (C) Confocal microscopy images of rhodamine-labeled stress fibres of hCFs infected monolayers with GFP-expressing PAO1 wild-type strain, at MOI=100 for 3h, compared to non-infected monolayers (control). Figure shows the red channel and the merged with the green channel visualizing the GFP-expressing bacteria. White arrows denote the stress fibres disassembly caused by PAO1-hCF invasion, which were strongly detected when the sample was nyquisted.

Figure 7. Bacterial survival and replication inside corneal fibroblasts

hCF monolayers were challenged with PAO1 bacteria for 24h. Gentamicin was added 3h post challenge to preserve the cells for the 24h duration. The number of intracellular bacteria was assessed at 3, 6, 9 and 24h post challenge. The number of recovered internalised bacteria increased significantly over time, indicating that PAO1 bacteria survive and replicate inside corneal fibroblasts. The bars represent the

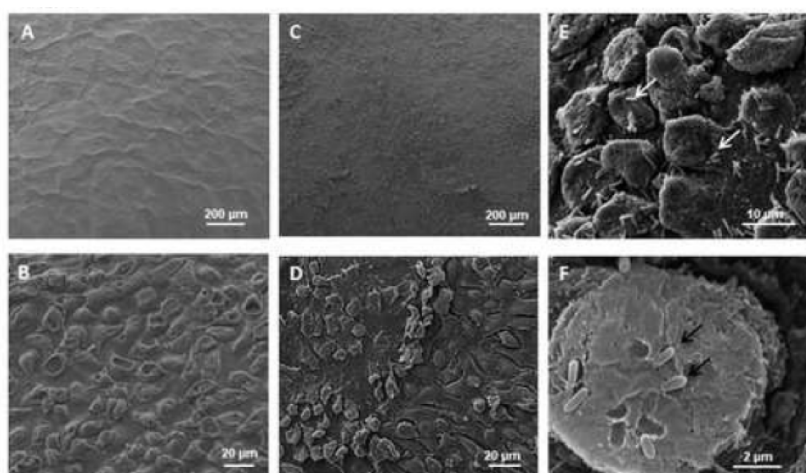
number of retrieved bacteria, and the error bars represent the standard error of the mean from 3 independent experiments.

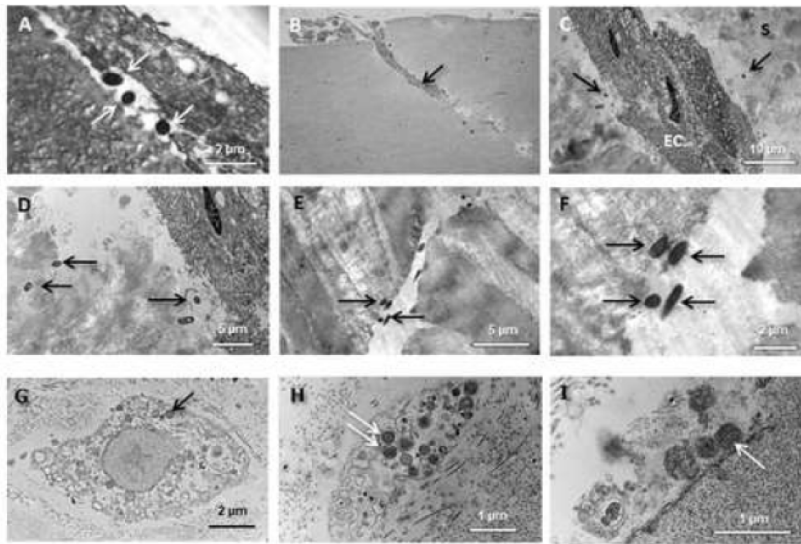
Figure 8. Cytotoxic effect of internalised PAO1 on human corneal fibroblasts

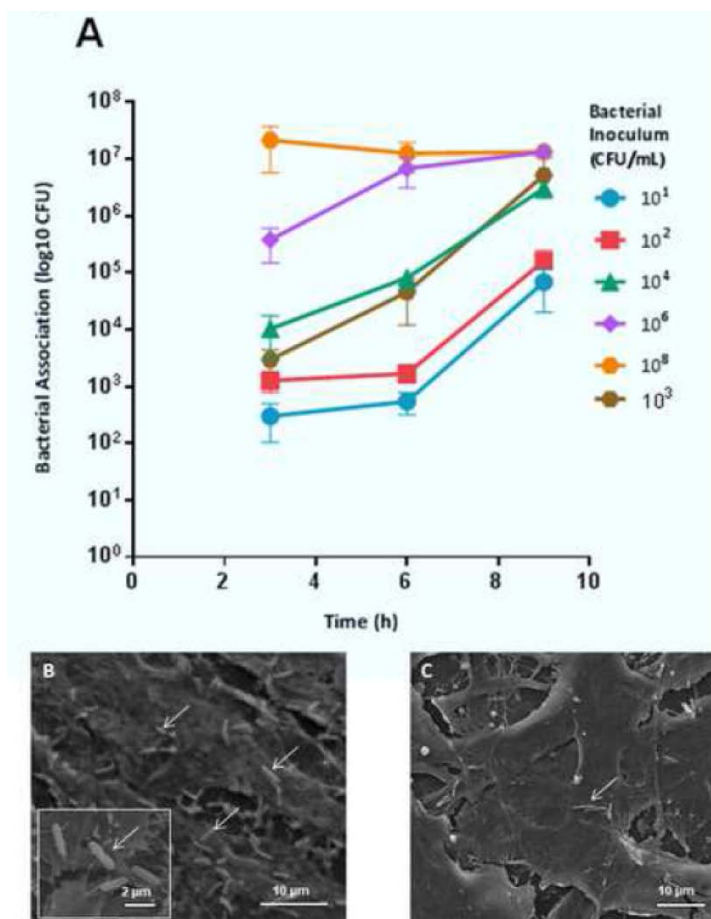
hCF monolayers were challenged at MOI 100 for 9 and 24h and gentamicin was added at 3h post challenge to preserve the fibroblasts for the duration of the experiment. LDH release in protected fibroblasts was similar to spontaneous release by unchallenged cells at 9h [A] and at 24h [B], contrary to unprotected cells. The data symbols and bars represent the mean value of LDH release percentage and number of retrieved bacteria, and the error bars represent the standard error of the mean from 3 independent experiments. The asterisks indicate statistically significant differences ($p < 0.05$)

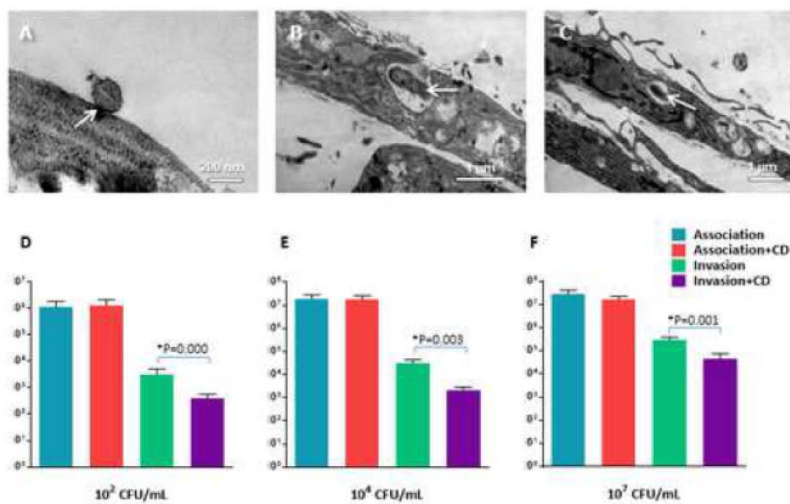
Table 1. Bacterial inocula and corresponding multiplicity of infection (MOI)

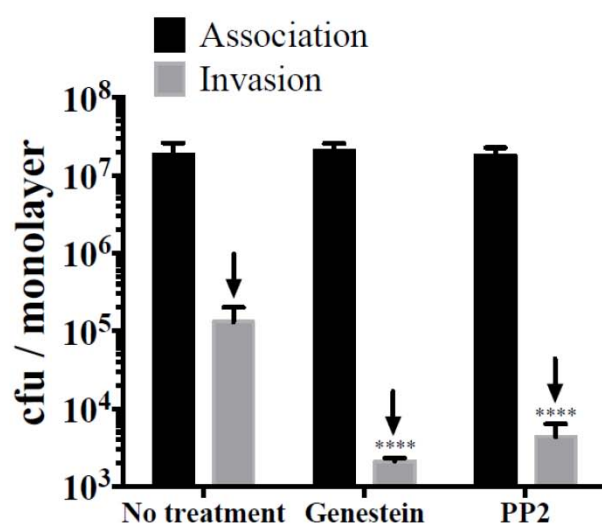
Bacterial inoculum (CFU/mL)	Multiplicity of infection (bacteria/cell)
10^1	0.0001
10^2	0.001
10^3	0.01
10^4	0.1
10^5	1
10^6	10
10^7	100
10^8	1000









(A)**(B)**